https://doi.org/10.31436/iiumej.v27i3.4626

Surface Treatment for Improved Electrochemical Performance of Activated Carbon Derived from Palm Empty Fruit Bunches

HASAN MARZUKI[1], ALYA NAILI ROZHAN[1*], MOHD HANAFI ANI[1], HADI PURWANTO[2]

[1]Department of Manufacturing and Materials Engineering, Kulliyyah of Engineering, International Islamic University Malaysia, 53100, Kuala Lumpur, Malaysia
[2] Department of Engineering Management, University of International Cement Indonesia UISI, Gresik, West Java 61122, Indonesia

**Corresponding author: alyanaili@iium.edu.my*

(Received: 23 July 2026; Accepted: 29 August 2026; Published online: 11 September 2026)

ABSTRACT: Recent interests in sustainable and green technologies for energy storage systems require extensive research to develop sustainable electrode materials. This includes developing biomass-derived activated carbons. In this research, empty fruit bunch (EFB) has been selected as the precursor material to produce activated carbon by the physical activation method, performed at 500 °C to 800 °C. Subsequently, a surface treatment process was performed using nitric acid to introduce oxygen functional groups. This step further improved the electrochemical properties of the EFB-based activated carbon material. The resulting samples were analyzed using Fourier transform infrared spectroscopy (FTIR), Raman spectroscopy, and X-ray photoelectron spectroscopy (XPS). The electrochemical performance was examined through cyclic voltammetry (CV), galvanostatic charge–discharge, and electrochemical impedance spectroscopy (EIS). FTIR analysis confirmed successful incorporation of oxygen functional groups, enhanced surface wettability, and improved electrolyte penetration. CV measurements showed a significant increase in the specific capacitance after treatment. Surface treatment of the activated carbon positively impacted all samples. The largest percentage increase was observed in sample AC ST 500, with a 71% increase in specific capacitance from 24 F g^{-1} to 71 F g^{-1}. AC ST 800 displayed the highest overall capacitance after surface treatment, at 183 F g^{-1}, a 9% increase from 166 F g^{-1} before surface treatment. This result shows that adding oxygen functional groups improves these properties by increasing surface wettability, which increases ion penetration within the activated carbon.

ABSTRAK: Minat yang semakin meningkat terhadap teknologi mampan dan hijau bagi sistem penyimpanan tenaga memerlukan penyelidikan menyeluruh bagi membangunkan bahan elektrod mampan, termasuk karbon teraktif berasaskan biojisim. Dalam kajian ini, tandan buah kosong (TBK) dipilih sebagai bahan pelopor bagi menghasilkan karbon teraktif melalui kaedah pengaktifan fizikal pada suhu antara 500 °C hingga 800 °C. Seterusnya, rawatan permukaan menggunakan asid nitrik dijalankan bagi menerapkan kumpulan berfungsi yang mengandungi oksigen dan seterusnya meningkatkan sifat elektrokimia bahan karbon teraktif berasaskan TBK. Sampel terhasil dianalisis menggunakan spektroskopi inframerah transformasi Fourier (FTIR), spektroskopi Raman dan spektroskopi fotoelektron sinar-X (XPS), manakala prestasi elektrokimia ini dinilai melalui voltametri berkitar (CV), pengecasan–nyahcas galvanostatik dan spektroskopi impedans elektrokimia (EIS). Analisis FTIR mengesahkan kejayaan penerapan kumpulan berfungsi yang mengandungi oksigen, peningkatan kebolehbasahan permukaan dan penembusan elektrolit yang lebih baik. Pengukuran CV menunjukkan peningkatan ketara dalam kemuatan tentu selepas rawatan

permukaan, dengan kesan positif diperhatikan pada semua sampel. Peningkatan peratusan terbesar dicatat pada sampel AC ST 500, dengan kemuatan tentu meningkat kira-kira 71%, daripada 24 F g^{-1} kepada 71 F g^{-1}. Sampel AC ST 800 pula mencatatkan kemuatan tentu keseluruhan tertinggi selepas rawatan permukaan, iaitu 183 F g^{-1}, bersamaan peningkatan kira-kira 9% daripada 166 F g^{-1} sebelum rawatan. Dapatan ini menunjukkan bahawa penerapan kumpulan berfungsi yang mengandungi oksigen dapat meningkatkan prestasi elektrokimia karbon teraktif dengan memperbaiki kebolehbasahan permukaannya, sekaligus meningkatkan penembusan ion ke dalam struktur karbon teraktif.

KEYWORDS: *Empty fruit bunch, activated carbon, physical activation, acid surface treatment, supercapacitor*

1. INTRODUCTION

Interest in developing sustainable, green energy storage system technologies has grown, as these systems are expected to have long life cycles, high performance, and be driven by low-carbon life cycle materials. This approach ensures that both high performance and minimal adverse environmental impact can be achieved [1]. Supercapacitors are promising energy storage systems that can deliver high performance due to their high cycling stability and power density. However, most commercially available supercapacitors use conventional carbon-based electrode materials derived from non-renewable fossil fuels.

In energy storage systems, demand for sustainable materials has increased, making renewable biomass materials an attractive alternative because of their strong potential as raw materials. Biomass-derived activated carbon has generated significant interest as a more economical and environmentally friendly substitute for conventional activated carbon [2]. This type of carbon, derived from natural resources, reduces dependence on non-renewable carbon sources. However, when meeting the performance demands of energy storage systems such as supercapacitors and batteries, these biomass-based materials often lack the required properties [3].

One abundantly available biomass source with strong potential for energy storage systems is palm empty fruit bunch (EFB) [4, 5]. Numerous studies have focused on optimizing synthesis parameters to produce high-performance activated carbon [6, 7]. However, many still produce activated carbon with relatively low electrochemical performance. Therefore, other techniques to improve electrochemical properties, such as surface treatment and element doping, need further exploration [8, 9].

Acid treatment is one feasible method to improve the efficiency of these biomass-derived activated carbons. This surface treatment adds functional groups, improving the surface characteristics of biomass-carbon materials. This improves ionic transport and the interface between the carbon materials and the electrolyte, which helps increase energy storage capacity [10]. Table 1 shows the effect of the acid treatment on the electrochemical properties of activated carbon.

Despite this development, we still need to fully understand how acid treatment influences the electrochemical performance of activated carbon, especially from agricultural biomass such as EFB. This is because few studies have demonstrated the effect of acid surface treatment on the electrochemical performance of activated carbon derived from agricultural biomass such as EFB. Table 1 shows that surface treatment greatly improved conventional materials such as commercial activated carbon, tire, and polymer, while the performance of palm kernel shell after surface treatment was relatively poor. A critical observation is that the surface-treatment

https://doi.org/10.31436/iiumej.v27i3.4626

methodology is similar for these biomass and conventional materials, which employ acid surface treatment at elevated temperatures. This is because the structure of biomass materials differs from that of conventional materials; therefore, a similar approach may not be practical. To address this gap, this study focuses on acid surface treatment of biomass material at room temperature.

Table 1. Literature data on the electrochemical properties of activated carbon before and after surface treatment

Raw Material	Surface Treatment Method	Specific Capacitance Before Surface Treatment (Fg^{-1})	Specific Capacitance After Surface Treatment (Fg^{-1})	Ref
Scrap Tire	30% nitric acid at 50 °C	188	190	[11]
Polyaniline	Concentrated nitric acid at 60 °C	50	350	[12]
Palm kernel shell	30% nitric acid at 60 – 80 °C	45	Less than 45	[13]
Commercial Activated Carbon	Ammonium persulfate and nitric acid at 60 °C	35	140	[14]
Commercial Activated Carbon	Nitric acid at 120 °C	142.47	229.17	[15]

In our previous study [16], we successfully converted EFB into activated carbon via physical and chemical activation methods. Their electrochemical performances have been examined. Therefore, this present study further explores how acid surface treatment affects the electrochemical properties of EFB. The effect of acid treatment is demonstrated by comparing the properties of activated carbon derived from EFB before and after acid surface treatment.

2. EXPERIMENTAL METHODS

2.1. Experiment

EFB was used as the raw material and was first prepared by pulverizing and drying it in an oven at 105°C for 24 hours to remove moisture. After drying, a two-step process converted the EFB into activated carbon. Initially, EFB was pyrolyzed at 500°C with a heating rate of 10°C/min in an argon atmosphere, with a residence time of 1 hour. This process yields solid carbon in the form of biochar. Next, the resulting biochar was activated to produce high-quality activated carbon via physical activation at 500°C, 600°C, 700°C, and 800°C, with a heating rate of 10°C/min and a flowing CO2 gas flow rate of 0.3 L/min. The residence time was one hour. CO_2 acted as the oxidizing agent in this process. This physical activation of the biochar to produce activated carbon was followed by a surface modification treatment using acid treatment.

Surface modification treatment enhances activated carbon by adding oxygen-containing functional groups to its surface. In this process, the activated carbon was soaked in 40 mL of 65% nitric acid for one hour at room temperature. Afterward, it was thoroughly rinsed with distilled water to remove any remaining acid, then dried at 105 °C for 24 hours in an oven to complete the treatment. The samples were categorized by treatment. Samples without surface modification were labeled as AC 500, AC 600, AC 700, and AC 800. Samples with surface modification were identified as AC ST 500, AC ST 600, AC ST 700, and AC ST 800.

https://doi.org/10.31436/iiumej.v27i3.4626

2.2. Physical Characterization

To evaluate the physical properties before and after surface modification, activated carbon was characterized using Fourier transform infrared spectroscopy (FTIR), X-ray photoelectron spectroscopy (XPS), and Raman spectroscopy. The defect structure of the activated carbon was evaluated by the ID/IG ratio in the Raman spectra. FTIR analysis was performed to examine the surface functional groups of the activated carbon derived from EFB, while XPS was used to identify and quantify these groups, complementing the FTIR analysis.

2.3. Preparation of Electrode

For slurry preparation, activated carbon was mixed with graphite as a conductive additive and polytetrafluoroethylene (PTFE) as a binder. A ratio of 8:1:1 was used, and the mixture was stirred well to achieve good homogeneity. Stainless steel mesh was selected as the current collector. It was cut into 1 cm x 1 cm pieces. Finally, 0.01 g of the slurry was hot-pressed onto the mesh at 10 MPa and 80°C.

2.4. Electrochemical Analysis

For electrochemical measurements, a Metrohm Autolab electrochemical workstation was used with a three-electrode setup in a 6 M KOH aqueous solution. In this setup, the activated carbon electrode, graphite, and an Ag/AgCl electrode served as the working, counter, and reference electrodes, respectively. The cyclic voltammetry (CV) potential window was tested from -0.8 to 0.4 V at a scan rate of 2 mV/s. The specific capacitance was calculated from the CV test using the equation below [17].

$$C_P = \frac{A}{2mk(\Delta V)} \tag{1}$$

where C_p is the specific capacitance, A is the area inside the CV curve, m is the mass of activated carbon, k is the scan rate, and ΔV is the potential window.

The voltage range for the galvanostatic charge and discharge (GDC) test was -0.8 to 0.1 V with a current density of 0.1 A/g. Electrochemical impedance spectroscopy (EIS) test was carried out with a frequency range of 100 kHz to 10 mHz with an amplitude of 10 mV.

In addition, this research uses a similar approach to electrode preparation and electrochemical test setup. This shows that the methodology adopted in this research is consistent with established published literature [18].

3. Results and Discussion

The acid surface treatment introduced oxygen-containing functional groups such as carbonyl, carboxyl, and hydroxyl on the activated carbon surface. Figure 1 illustrates the mechanism of the activated carbon synthesis via physical activation and the surface treatment of the activated carbon [19]. This illustration also explains the mechanism of each process, including how surface treatment enhances the surface wettability of activated carbon to facilitate electrolyte movement and increase the efficiency of ion penetration within the activated carbon networks [20].

FTIR analysis showed functional groups on the activated carbons. The wavenumbers 2400 to 3600 cm^{-1}, 1710 cm^{-1}, and 1500 cm^{-1} indicated the presence of O-H, C=O, and C=C functional groups, respectively, while the wavenumbers 1205 cm-1 and 1103 cm-1 indicated the presence of the C-O functional group [21]. Figure 2 shows the FTIR spectra of the activated carbon before and after surface treatment. The peak at the representative wavenumber of the

https://doi.org/10.31436/iiumej.v27i3.4626

surface functional group increased. This observation indicated that the surface treatment had successfully introduced oxygen functional groups on the surface of the activated carbon. The amount of functional groups developed on the surface of activated carbon varied among the samples, although constant parameters of the surface treatment process were being applied. This could be due to the original physical properties of activated carbon during the physical activation process.

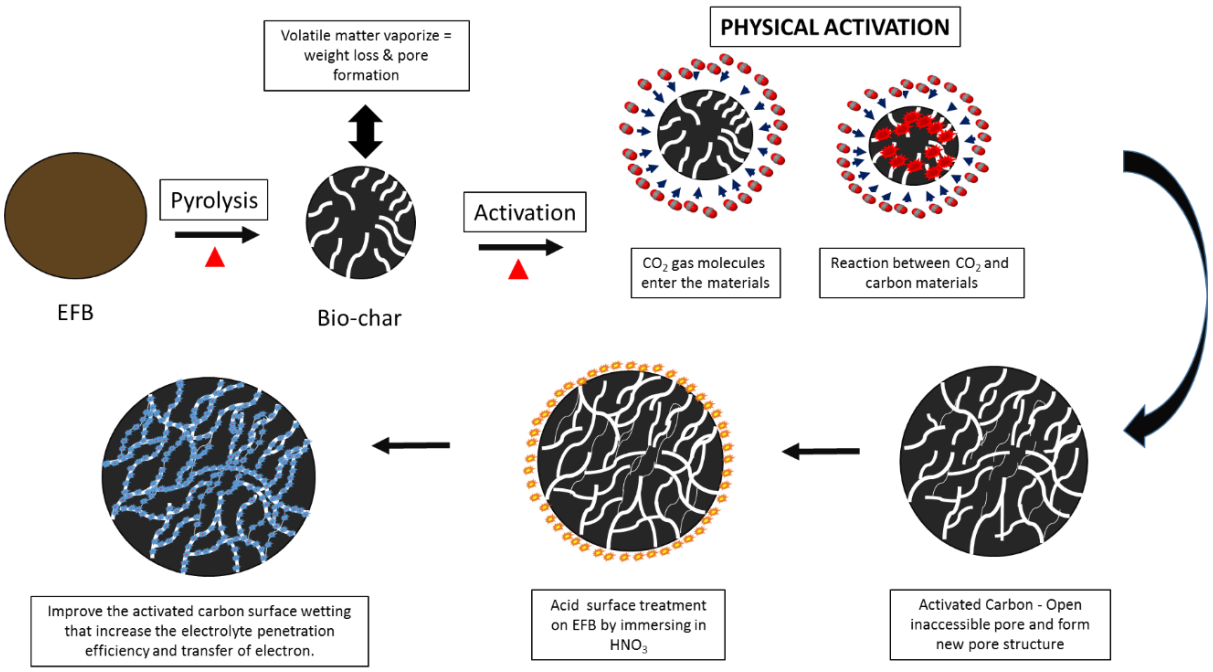

Figure 1. Synthesis pathways of the activated carbon from biomass

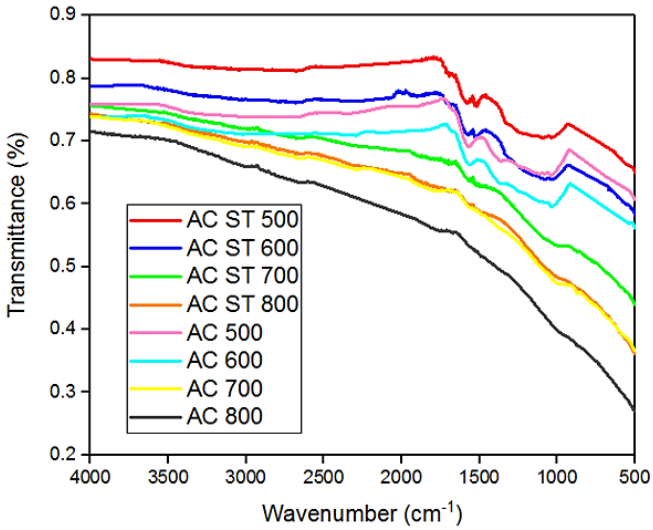

Figure 2. FTIR spectra of activated carbon before and after surface treatment

XPS analysis was conducted on AC ST 800 to support the FTIR findings, since AC ST 800 showed fewer FTIR peaks than the other surface-treated samples. Figure 3 shows a peak in the XPS spectra representing C-O, C=O, and O-C=O. From the XPS analysis, the surface functionality present on the activated carbon sample can be quantified as shown in Table 2. This quantitative analysis of functional-group percentages better verifies surface functional-group presence after surface treatment [22].

https://doi.org/10.31436/iiumej.v27i3.4626

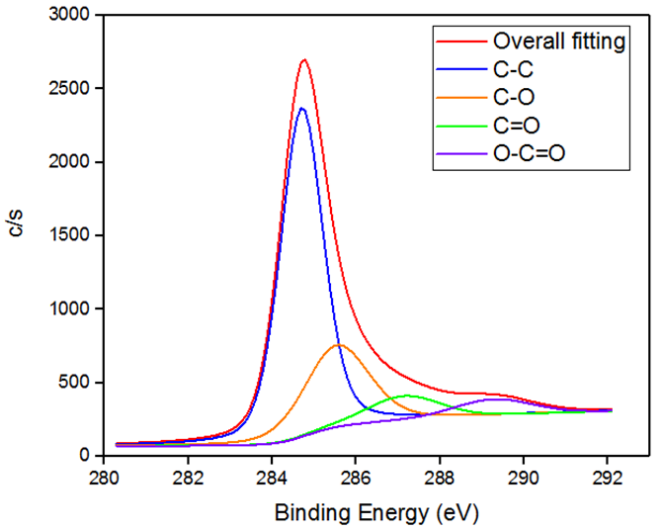

Figure 3. XPS spectra of AC ST 800

Table 2. Surface functional groups on AC ST 800

Sample	AC ST 800
C-C (%)	63.10
C-O (%)	23.41 – 63.15
C=O (%)	8.03 – 33.55
O-C=O (%)	3.31 – 5.55

Structural defects in activated carbon materials play an important role in determining their electrochemical performance. Raman spectroscopy analysis was used to analyze the structural defects in the samples. Characterizing defects is important for understanding the relationship between structural defects within the activated carbon network and its electrochemical performance. Although a higher defect density in carbon materials increases the density of electronic states and can lead to higher capacitance, structural defects in activated carbon are not the only factor affecting electrochemical performance. Other factors also contribute to the electrochemical properties of activated carbon, such as surface area, pore connectivity, and surface wettability [23].

Defects in carbon materials can be analyzed from the I_D and I_G of the Raman spectra, where a higher ID/IG indicates a higher defect structure. The D and G bands corresponding to activated carbon are 1348 cm^{-1} and 1600 $cm^{-1,}$ respectively [24]. Figure 4 illustrates the Raman spectra of AC ST 500 and AC ST 800, the samples with the highest and lowest functional group peaks in the FTIR spectra, along with the untreated samples, AC 500 and AC 800.

Table 3 compares the ID/IG ratios of the Raman spectra of the activated carbon before and after surface treatment. The I_D/I_G ratios for the samples showed no major differences. This suggests that the surface treatment in this experiment did not significantly affect the activated carbon's defect structure. The I_D/I_G ratio increased slightly for AC ST 500, while it remained unchanged for AC ST 800. The I_D/I_G values of AC ST 500 and AC ST 800 were also in a similar range, indicating that structural defects may not be a major factor in determining the electrochemical properties of activated carbon after surface treatment.

https://doi.org/10.31436/iiumej.v27i3.4626

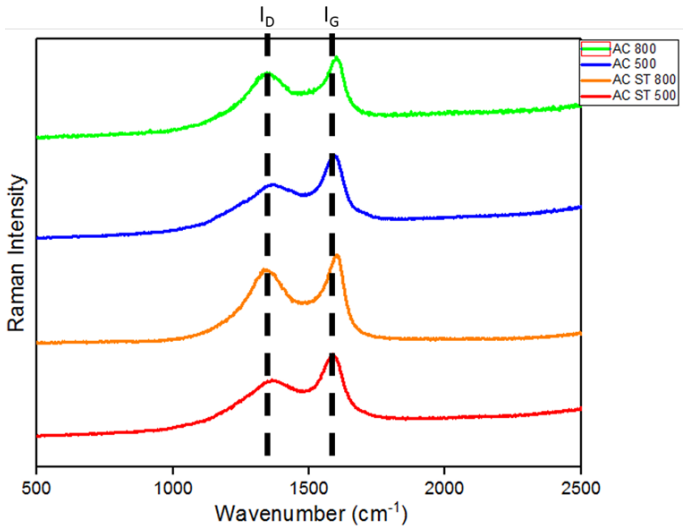

Figure 4. Raman spectra of activated carbon before and after surface treatment

Table 3. ID/IG of the activated carbon before and after surface treatment

Sample	I_D/I_G
AC 500	0.70
AC ST 500	0.73
AC 800	0.84
AC ST 800	0.84

Figure 5 shows the CV curve for activated carbon before and after surface treatment. The area under a CV curve represents the specific capacitance of the activated carbon; a larger area indicates higher specific capacitance. The CV curve shape can also be used to analyze the electrochemical energy storage mechanism. A perfect square CV curve indicates a purely electrochemical double-layer mechanism, without any pseudocapacitive reaction. All samples, before and after surface treatment, did not show a perfect square curve, indicating that some pseudocapacitive reactions occurred [25]. This observation may be related to the FTIR spectra in Figure 2, which showed that all samples had a peak indicating an oxygen functional group, typical of biomass carbon-based materials with traces of functional-group impurities. The surface treatment on activated carbon was applied to determine whether the electrochemical properties could be improved or negatively affected by adding functional groups from the treatment. Figure 5 shows that all CV curves improved after surface treatment, indicating that the surface treatment process used in this research is compatible with activated carbon derived from EFB via physical activation. Table 4 compares the specific capacitance of activated carbon before and after surface treatment.

As shown in Table 4, all samples increased in specific capacitance after surface treatment, indicating that introducing oxygen functional groups using the method applied in this study did not collapse the activated carbon structure, which could otherwise negatively affect capacitance [13]. The specific capacitance of activated carbon increased from AC 500 to AC 800 before surface treatment, which was attributed to the activation temperature, as higher temperatures produced activated carbon with greater specific capacitance. AC 800, activated at 800 °C, produced the highest capacitance. After surface treatment, the same trend held: AC ST 800 produced the highest capacitance. However, the percentage change in specific capacitance before and after treatment followed an inverse pattern, with AC ST 500 showing the highest percentage increase, which gradually decreased toward AC ST 800. FTIR analysis supported

https://doi.org/10.31436/iiumej.v27i3.4626

this pattern: AC ST 500 showed the highest peak for oxygen functional groups, which led to greater wettability improvement. This resulted in a higher percentage increase in capacitance. While wettability enhances electrolyte penetration, it does not change the activated carbon structure, such as pore connectivity, surface area, and structural defects, that play major roles in electrochemical performance [26]. Although AC ST 800 has the lowest oxygen functional group content after surface treatment, it still showed the highest overall specific capacitance, which was contributed by the original properties of the activated carbon prior to surface treatment. Introducing oxygen functional groups enhanced its capacitance. This indicates that the overall effect depends heavily on the activated carbon's structural properties [27].

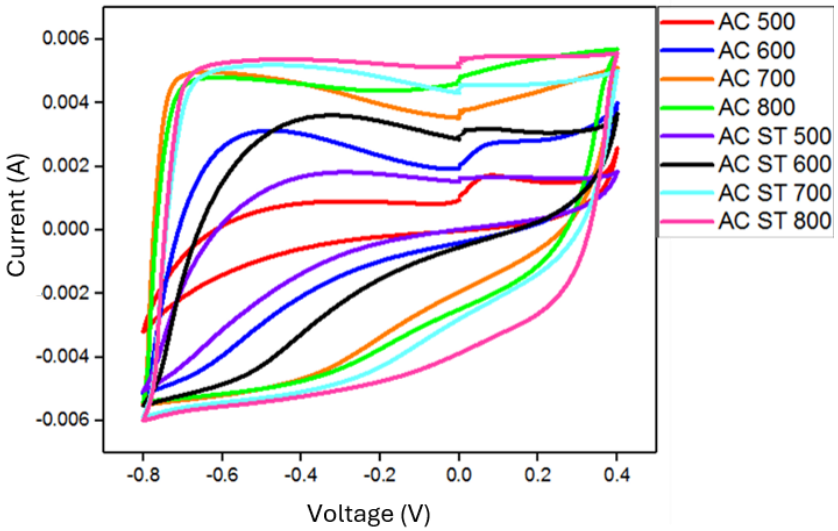

Figure 5. CV curve for activated carbon before and after surface treatment

Table 4. Specific capacitance of activated carbon before and after surface treatment

Sample	Specific Capacitance, Cp (Fg^{-1})	Sample	Specific Capacitance, Cp (Fg^{-1})	Percentage Difference (%)
AC 500	24.72	AC ST 500	42.35	71.32
AC 600	76.00	AC ST 600	88.59	16.57
AC 700	146.60	AC ST 700	161.84	10.40
AC 800	166.68	AC ST 800	183.03	9.73

Figure 6 shows the galvanostatic charge-discharge (GCD) curve, which illustrates the charging and discharging behavior of the activated carbon electrode during energy storage. This curve also shows ion diffusion mobility, represented by the voltage drop after the peak. The discharging time of AC ST 800 was higher than that of AC 800. A longer discharge time indicates greater electrolyte-ion involvement during discharge [28]. Greater electrolyte-ion involvement indicates ion movement within the activated carbon pore network. This can be attributed to surface functional groups, which enhance the wettability and hydrophilicity of the activated carbon surface. Improved surface wettability and hydrophilicity can enhance ion movement, as shown by the charging and discharging times in the GCD analysis of activated carbon [29, 30].

https://doi.org/10.31436/iiumej.v27i3.4626

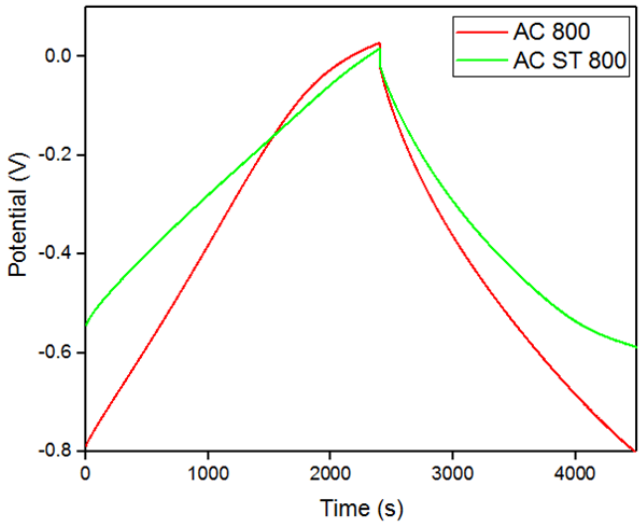

Figure 6. Galvanostatic charge-discharge (GCD) curve of AC 800 and AC ST 800

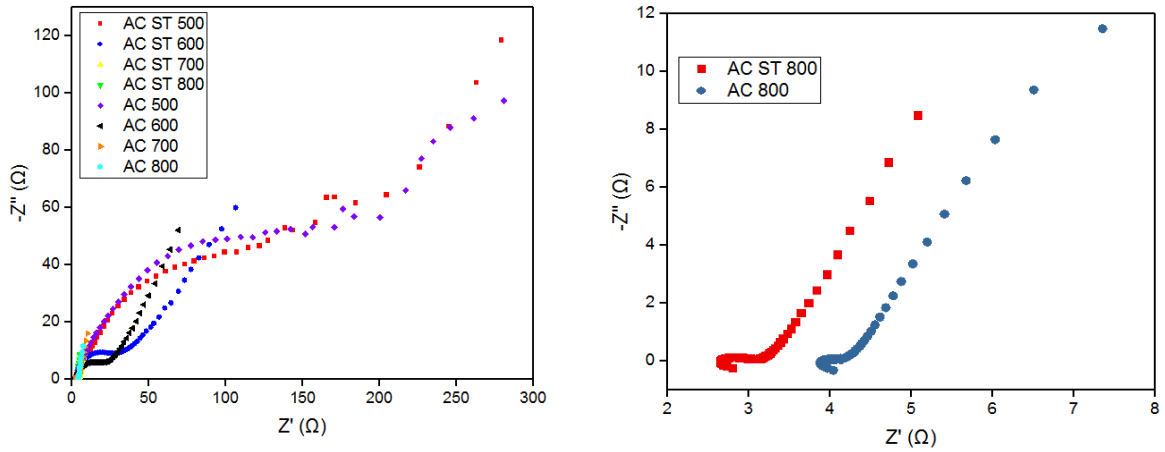

Figure 7. Nyquist plots of a) activated carbon before and after surface treatment; b) AC 800 and AC ST 800

Figure 7 shows the Nyquist plots of the EIS analysis. These Nyquist plots allow determination of the activated carbon resistance. These values were determined by evaluating the semicircle in the plots, which represents the electrolyte resistance at the electrode interface (R_S), the internal resistance of the activated carbon electrode (R_P), and the equivalent series resistance (ESR) of the activated carbon electrode. The values of R_S, R_P, and ESR were represented by the start of the semicircle, the end of the semicircle, and the diameter of the semicircle ($R_P - R_S$), respectively [31]. From the Nyquist plot, activated carbon samples with higher specific capacitance show lower resistance values.

Table 5. ESR value of activated carbon before and after surface treatment

Sample	ESR (Ω)	Sample	ESR (Ω)	Percentage Difference (%)
AC 500	153.96	AC ST 500	155.21	0.81
AC 600	18.96	AC ST 600	25.39	22.91
AC 700	1.25	AC ST 700	1.02	-18.40
AC 800	0.10	AC ST 800	0.31	244.44

https://doi.org/10.31436/iiumej.v27i3.4626

Several factors influence the resistance value, including pore characteristics and surface area, defect structure, and the presence of functional groups. In addition, these ESR values can also indicate the behavior of the carbon-based supercapacitor. Typical ESR values for carbon electrode supercapacitors range from 0.134 to 1.149 [32]. Based on Table 5, some activated carbon samples showed decreased ESR, while others increased. Notably, the ESR values for samples AC ST 700 and AC ST 800 remained below 1.149 Ω after surface treatment. Although AC ST 800 showed an increase in ESR, this can be attributed to its initially low ESR, where even a slight increase resulted in a relatively larger percentage increment. The AC ST 700 and AC ST 800, which exhibited higher specific capacitance and lower resistance, proved that with the right combination of the physical activation parameter, a better electrochemical performance could be achieved, and the addition of the oxygen functional group would enhance its specific capacitance while not compromising the internal resistance for the electrolyte and ionic movement within the activated carbon network [22].

Meanwhile, the other segment of the Nyquist plot, the straight line after the semicircle, represents the resistive and capacitive behavior of ions penetrating the activated carbon pores. Therefore, this steep slope indicates efficient ion penetration into the pore networks of activated carbon [33]. For AC ST 600, AC ST 700, and AC ST 800, the slopes were similar, while AC ST 500 showed a significant difference after Z' = 200 Ω, which may also be related to its large change in specific capacitance. This suggests better ion penetration, which led to improved capacitance performance [25].

4. CONCLUSION

This research compares the physical properties and electrochemical performance of activated carbon before and after surface treatment prepared by physical activation. The main conclusions drawn from this research are as follows:

1. The amount of the oxygen functional group developed during surface treatment varied among the samples, although the same treatment parameters were applied. This subsequently led to different electrochemical performance rates.
2. The Raman spectroscopy analysis showed that the surface treatment did not have major impacts on the structural defects of the activated carbon.
3. All samples exhibited a positive increment in specific capacitance after the surface treatment. This indicated that the surface treatment process and parameters used in this study did not cause collapse of the activated carbon structure and, consequently, lower electrochemical performance.
4. Although AC ST 500 recorded the highest amount of oxygen functional groups developed, and translated to the highest specific capacitance increase, it still has the lowest specific capacitance value as compared to the other samples. This is because the overall structure of the activated carbon, such as surface area, porosity, and structural defects developed during the physical activation process, still plays a major role in shaping the electrochemical properties of the activated carbon, while the addition of oxygen functional groups contributed mainly to enhancing those properties.
5. While there were samples that exhibited an increase in the resistance value, this did not have major implications for the electrochemical performance, as all the samples showed a positive increase in the specific capacitance.

REFERENCES

[1] Rustamaji H, Prakoso T, Devianto H, Widiatmoko P, Kurnia KA (2023) Facile synthesis of N, S-modified activated carbon from biomass residue for promising supercapacitor electrode applications. Bioresour. Technol. Rep., 21:101301.

[2] Ferdous AR, Shah SS, Shaikh MN, Barai HR, Marwat MA, Oyama M, Aziz MA (2024) Advancements in biomass-derived activated carbon for sustainable hydrogen storage: A comprehensive review. Chem. Asian J., 19(16):e202300780.

[3] Lobato-Peralta DR, Okoye PU, Alegre C (2024) A review on carbon materials for electrochemical energy storage applications: State of the art, implementation, and synergy with metallic compounds for supercapacitor and battery electrodes. J. Power Sources, 617:235140.

[4] Rozhan AN, Ani MH, Salleh HM, Akiyama T, Purwanto H (2015) Development of carbon-infiltrated bio-char from oil palm empty fruit bunch. ISIJ Int., 55(2):436-440.

[5] Purwanto H, Salleh HM, Rozhan AN, Mohamad AS, Zakiyuddin A (2018) Phase change of iron ore reduction process using EFB as reducing agent at 900-1200C. IOP Conf. Ser. Mater. Sci. Eng., 342:012054.

[6] Choi MS, Park S, Lee H, Park HS (2018) Hierarchically nanoporous carbons derived from empty fruit bunches for high performance supercapacitors. Carbon Lett., 25:103-112.

[7] Nasir S, Hussein MZ, Zainal Z, Yusof NA (2018) Carbon-based nanomaterials/allotropes: A glimpse of their synthesis, properties and some applications. Materials, 11(2):1-24.

[8] Jha MK, Joshi S, Sharma RK, Kim AA, Pant B, Park M, Pant HR (2021) Surface modified activated carbons: Sustainable bio-based materials for environmental remediation. Nanomaterials, 11:3140.

[9] Malini K, Selvakumar D, Kumar NS (2023) Activated carbon from biomass: Preparation, factors improving basicity and surface properties for enhanced CO2 capture capacity – A review. J. CO2 Util., 67:102318.

[10] Petrovic B, Gorbounov M, Soltani SM (2022) Impact of surface functional groups and their introduction methods on the mechanisms of CO2 adsorption on porous carbonaceous adsorbents. Carbon Capture Sci. Technol., 3:100045.

[11] Han Y, Zhao PP, Dong XT, Zhang C, Liu SX (2014) Improvement in electrochemical capacitance of AC from scrap tires by nitric acid treatment. Front. Mater. Sci., 8(4):391-398.

[12] Wei X, Jiang X, Wei J, Gao S (2015) Functional groups and pore size distribution do matter to hierarchically porous carbons as high-rate-performance supercapacitor. Chem. Mater., 28(2):445-458.

[13] Arango DI, Zapata-Benabithe Z, Arenas EC, Perez-Osorno JC (2018) Influence of surface modification with nitric acid on electrochemical performance of agroindustrial waste-based AC. J. Mater. Sci. Mater. Electron., 29(18):15557-15569.

[14] Liu C, Koyyalamudi BB, Li L, Emani S, Wang C, Shaw LL (2016) Improved capacitive energy storage via surface functionalization of AC as cathodes for lithium ion capacitors. Carbon, 109:163-172.

[15]] Zhang C, Wei YL, Cao PF, Lin MC (2018) Energy storage system: Current studies on batteries and power condition system. Renew. Sustain. Energy Rev., 82:3091-3106.

[16] Marzuki H, Rozhan AN, Purwanto H (2024) Electrochemical performance of activated carbon derived from empty fruit bunch via chemical and physical activation methods. J. Kejuruteraan, 36(4):1437-1450.

[17] Darkwa MK, Zquine C, Kahol PK, Gupta RK (2019) Novel biomass-derived smoke-like carbon as a supercapacitor electrode material. R. Soc. Open Sci., 6(7):190132.

[18] Haitao S, Qiang Q, Zhuangzhuang Y, Yanrong Z, Ling Q, Yibo Z, Chenguang L, Mingqiang Z, Xuanmin Y (2025) Supercapacitor performance of activated carbon from Eucommia ulmoides Oliver wood optimized by the activation method. ACS Omega, 10:15368-15380.

[19] Figueiredo JL (2018) Nanostructured porous carbons for electrochemical energy conversion and storage. Surf. Coat. Technol., 350:307-312.

[20] Sarwar A, Ali M, Khoja AH, Nawar A, Waqas A, Liaquat R, Asjid M (2021) Synthesis and characterization of biomass-derived surface-modified AC for enhanced CO2 adsorption. J. CO2 Util., 46:101476.

[21] Shi G, Liu C, Wang G, Chen X, Li L, Jiang X, Zhang H (2018) Preparation and electrochemical performance of biomass-based AC nanofibers. Ionics, 25(4):1805-1812.

[22] Yang W, He W, Zhang F, Hickner MA, Logan BE (2014) Single-step fabrication using a phase inversion method of poly(vinylidene fluoride) (PVDF) AC air cathodes for microbial fuel cells. Environ. Sci. Technol. Lett., 1(10):416-420.

[23] Zheng Y, Deng T, Yue N, Zhang W, Zhu X, Yang H, Zheng W (2021) Raman spectroscopy and correlative-Raman technology excel as an optimal stage for carbon-based electrode materials in electrochemical energy storage. J. Raman Spectrosc., 52(12):2119-2130.

[24] Singh A, Ghosh K, Kumar S, Agarwal AK, Jassal M, Goswami P, Chaturvedi H (2019) Interdigitated flexible supercapacitor using AC synthesized from biomass for wearable energy storage. arXiv:1903.02384.

[25] Frackowiak E, Béguin F (2001) Carbon materials for the electrochemical storage of energy in capacitors. Carbon, 39(6):937-950.

[26] Olivares-Marín M, Fernández-González C, MacÍas-García A, Gómez-Serrano V (2012) Preparation of AC from cherry stones by physical activation in air. Influence of the chemical carbonisation with H2SO4. J. Anal. Appl. Pyrolysis, 94:131-137.

[27] Dieu HTTD, Charoensook K, Tai HC, Lin YT, Li YY (2021) Preparation of activated carbon derived from oil palm empty fruit bunches and its modification by nitrogen doping for supercapacitors. J. Porous Mater., 28:9-18.

[28] Yu H, Wu J, Fan L, Xu K, Zhong X, Lin Y, Lin J (2011) Improvement of the performance for quasi-solid-state supercapacitor by using PVA-KOH-KI polymer gel electrolyte. Electrochim. Acta, 56(20):6881-6886.

[29] Taer E, Melisa M, Agustino A, Taslim R, Sinta MW, Apriwandi A (2021) Biomass-based AC monolith from Tectona grandis leaf as supercapacitor electrode materials. Energy Sources Part A Recovery Util. Environ. Eff., 1-12.

[30] Ishak MM, Deraman M, Dolah BNM, Othman MAR, Omar R, Basri NH, Aziz AA (2015) Effects of activation time on the performance of supercapacitor binderless AC electrodes derived from fibers of oil palm empty fruit bunches. Adv. Mater. Res., 1112:308-312.

[31] Farma R, Deraman M, Awitdrus, Talib IA, Omar R, Manjunatha JG, Dolah BNM (2013) Physical and electrochemical properties of supercapacitor electrodes derived from carbon nanotube and biomass carbon. Int. J. Electrochem. Sci., 8(1):257-273.

[32] Kim YJ, Lee BJ, Suezaki H, Chino T, Abe Y, Yanagiura T, Endo M (2006) Preparation and characterization of bamboo-based ACs as electrode materials for electric double layer capacitors. Carbon, 44(8):1592-1595.

[33] Chen WC, Wen TC (2003) Electrochemical and capacitive properties of polyaniline-implanted porous carbon electrode for supercapacitors. J. Power Sources, 117:273-282.